# Inversion of CMP Gathers for P and S Velocity.

*Peter Mora*

**Abstract**

A method for inverting common midpoint gather data for the parameters P-velocity, S-velocity, density, quality factor, and source waveform is described. The method uses an iterative nonlinear least squares formulation for overdetermined problems. Therefore, an efficient modeling theory is required to enable the required iterations of parameters to be carried out within a reasonable amount of time. The iterations proceed until a solution is located which minimizes the square error between the modeled and real data. The practical limitations are the ability of the modeling theory to simulate the real data, and the sizes of the data and parameter spaces which determine matrix dimensions and hence speed of the algorithm. A simple ray tracing scheme for horizontal layers is used as the modeling theory, and an inversion for P and S velocities in a 16 layer model is performed for synthetic data generated by the same modeling theory. The P and S velocities resulting from the inversion are in reasonably close agreement with the true values.

## Introduction

The classical nonlinear least squares problem for overdetermined systems can be solved using an iterative scheme (Tarantola 1982) such as

$$p_{k+1} = p_k + (g'^T_k C_d^{-1} g'_k + C_p^{-1})^{-1}[g'^T_k C_d^{-1}(d - g(p_k)) - C_p^{-1}(p_k - p_0)] \qquad (1)$$

where $p_k$ denotes the parameters after $k$ iterations with a priori covariances $C_p$; $d$ is the data with corresponding assigned covariances $C_d$; $g$ is the geophysical theory used to model the data and $g'$ is the partial derivatives of $g$ with respect to $p$. This gives a probabilistic least squares solution assuming that Gaussian probability density functions describe the data and parameter distributions. The essential requirement of the iterative inversion scheme given by equation (1), is a theory $g$ which is capable of adequately modeling the

data and is differentiable with respect to the parameters. For highly nonlinear functions $g$, local minima in the square error functional may be present. The problem of local minima may sometimes be overcome by adjusting covariances or solving using a number of different starting parameter sets $p_0$ ( Tarantola, 1983, pers. comm.).

I will consider a horizontally layered system where layer thickness is known, and formulate the inverse problem for parameters P-velocity, S-velocity, density, quality factor and source waveform. The assumption that layer thickness be known will not be a limitation in the inversion because the layers are sampled at the spatial equivalent of Nyquist frequency. The data is a Fourier transformed common midpoint gather so the geophysical modeling theory $g$, must be capable of modeling attenuative seismic waves at any propagation angle through the layers. Ray tracing is a fast reliable method, which for horizontal layers amounts to solving parametric summation equations for offset and traveltime as a function of ray parameter $P$. The complex ray amplitudes are computed by evaluating the complex reflection and transmission coefficient products, and an exponential term that includes both the linear traveltime phase shift and attenuation via Futterman's theory of 1962.

**Definitions**

The parameters are the variables being inverted, specifically the P-velocities, S-velocities, densities and quality factors of the layers and the source Fourier spectrum. Parameters are put into a partitioned column vector

$$p = \begin{bmatrix} p_1 \\ . \\ . \\ . \\ p_M \end{bmatrix} = \begin{bmatrix} \alpha \\ \beta \\ \rho \\ Q \\ S \end{bmatrix} = \begin{bmatrix} \begin{bmatrix} \alpha_1 \\ . \\ . \\ \alpha_L \end{bmatrix} \\ . \\ . \\ \begin{bmatrix} S_1 \\ . \\ . \\ S_W \end{bmatrix} \end{bmatrix} \qquad (2)$$

*where*, $p_m$ = *parameter m*

$\alpha$ = *column vector of P-velocities*

$\beta$ = *column vector of S-velocities*

$\rho$ = *column vector of densities*

$Q$ = *column vector of quality factors*

$S$ = *column vector of source spectrum*

The subscripts $l=1, \ldots, L$ is used for layer number and $w=1, \ldots, W$ denotes angular frequency. The data consists of Fourier transformed common midpoint traces arranged into a partitioned column vector

$$\mathbf{d} = \begin{bmatrix} d_1 \\ \cdot \\ \cdot \\ \cdot \\ d_N \end{bmatrix} = \begin{bmatrix} D_1 \\ \cdot \\ \cdot \\ \cdot \\ D_H \end{bmatrix} = \begin{bmatrix} \begin{bmatrix} D_{11} \\ \cdot \\ \cdot \\ D_{1W} \end{bmatrix} \\ \cdot \\ \cdot \\ \cdot \\ \begin{bmatrix} D_{H1} \\ \cdot \\ \cdot \\ D_{HW} \end{bmatrix} \end{bmatrix} \tag{3}$$

*where*, $d_n$ = *data* $n$

$D_h$ = *column vector of data at offset* $h$ = *Fourier transformed trace*

$D_{hw}$ = *data value at offset* $h$ *and angular frequency* $w$ = *value in a trace*

$d = g(p)$ = *geophysical theory* = *matrix structured identically to* $d$ *above but with* $g$ *and* $G$ *replacing* $d$ *and* $D$.

So far, the definitions are basic nomenclature specifying the parameter and data spaces and extensions to define the required matrix of partial derivatives $g'$ are given below.

$$g' = \frac{\partial g_n}{\partial p_m} = \begin{bmatrix} \partial_\alpha G_1 & \cdot\cdot & \partial_S G_1 \\ \cdot & & \cdot \\ \cdot & & \cdot \\ \partial_\alpha G_H & \cdot\cdot & \partial_S G_H \end{bmatrix}$$

$$= g' = \begin{bmatrix} \begin{bmatrix} \partial_{\alpha_1} G_{11} & \cdots & \partial_{\alpha_L} G_{11} \\ \vdots & & \vdots \\ \partial_{\alpha_1} G_{1W} & \cdots & \partial_{\alpha_L} G_{1W} \end{bmatrix} & \cdots & \begin{bmatrix} \partial_{S_1} G_{11} & \cdots & \partial_{S_V} G_{11} \\ \vdots & & \vdots \\ \partial_{S_1} G_{1W} & \cdots & \partial_{S_V} G_{1W} \end{bmatrix} \\ \vdots & & \vdots \\ \begin{bmatrix} \partial_{\alpha_1} G_{H1} & \cdots & \partial_{\alpha_L} G_{H1} \\ \vdots & & \vdots \\ \partial_{\alpha_1} G_{HW} & \cdots & \partial_{\alpha_L} G_{HW} \end{bmatrix} & \cdots & \begin{bmatrix} \partial_{S_1} G_{H1} & \cdots & \partial_{S_V} G_{H1} \\ \vdots & & \vdots \\ \partial_{S_1} G_{HW} & \cdots & \partial_{S_V} G_{HW} \end{bmatrix} \end{bmatrix} \tag{4}$$

**Modeling theory**

Parametric ray equations to solve for offset $h$ and traveltime $\tau$ as functions of ray parameter $P$ are used to model rays travelling through horizontal layers. Each ray has a complex amplitude that is the product of the source spectrum, the reflection and transmission coefficients, and an exponential term which contains the linear phase shift due to the traveltime delay plus the attenuation effects. The modeled data at offset $h$ and angular frequency $w$ is given by the sum of responses of all possible rays which travel an offset $h$; that is

$$G_{hw} = \sum_{ray} G_{h_{ray} w}$$

$$= \textit{modeled data for offset h and angular frequency w}$$

Neglecting ray spreading, the ray amplitude at angular frequency $w$ is

$$G_{h_{ray} w} = S_w \, U_{h_{ray} w} \, R_{h_{ray}} \, T^+_{h_{ray}} \, T^-_{h_{ray}}$$

$$= \textit{modeled data for a ray at frequency w traversing offset h}$$

*where*, $S$ = *source*

$U$ = *exponential terms including traveltime effect and attenuation*

$R$ = *complex elastic reflection coefficient product*

$T^+$ = *complex elastic transmission coefficient product (down)*

$T^-$ = *complex elastic transmission coefficient product ( up )*

For primary P reflection events only, the ray summation simplifies to

$$G_{hw} = \sum_{l=1}^{L} G_{h_l w} \tag{5}$$

$$and \quad G_{h_l w} = S_w \; U_{h_l w} \; R_{h_l} \; T^{+}_{h_l} \; T^{-}_{h_l} \tag{6}$$

$$where \quad T^{+}_{h_l} = \prod_{k=1}^{l-1} T^{+}_{h_l k} \tag{7}$$

$$T^{-}_{h_l} = \prod_{k=1}^{l-1} T^{-}_{h_l k} \tag{8}$$

$$R_{h_l} = R_{h_l} \tag{9}$$

$$U_{h_l w} = \exp[-w(i(\tau_{h_l} + \delta_w \gamma_{h_l}) + \gamma_{h_l})] \tag{10}$$

The subscript $h_l$ indicates a ray which is reflected from the base of the $l$-th layer and traverses offset $h$. The remaining terms are defined below.

$$\delta_w = \frac{2}{\pi} \ln\left(\frac{w}{w_0}\right) \tag{11}$$

$$\gamma_{h_l} = \sum_{k=1}^{l-1} t_{h_l k} / Q_k \tag{12}$$

$$\tau_{h_l} = 2 \sum_{k=1}^{l-1} t_{h_l k} \tag{13}$$

$$t_{h_l k} = \frac{z_k}{\alpha_k \cos\theta_{h_l k}} = \frac{z_k}{\alpha_k \sqrt{1 - (P_{h_l} \alpha_k)^2}} = \frac{z_k}{\alpha_k \sqrt{1 - A_k^{-2}}} \tag{14}$$

$$h_l = 2 \sum_{k=1}^{l-1} z_k \tan\theta_{h_l k} = 2 \sum_{k=1}^{l-1} \frac{z_k}{\sqrt{(P_{h_l} \alpha_k)^{-2} - 1}} = 2 \sum_{k=1}^{l-1} z_k / \sqrt{A_k^2 - 1} \tag{15}$$

$$where \quad P = P_{h_l} = P_h(\alpha_1, \ldots, \alpha_l) = \frac{\sin\theta_{h_l k}}{\alpha_k} \tag{16}$$

$$and \quad A_k = \frac{1}{P \alpha_k} \tag{17}$$

The angular frequency $w_0$ is the the quality factor reference frequency used in Futterman's almost constant Q dispersion theory.

**Computation of partial derivatives**

The partial derivative matrix $g'$ is defined by equations (4) through (17) and c be easily computed while performing the modeling for the case of ray tracing. The derivatives of $g_n$ with respect to parameter $p_m$ are required for a ray which travels a horizontal distance equal to the specified constant offset $h$. We have the ray amplitude function

$$G_{h_l} = G(P_h(\alpha_1, \ldots, \alpha_l), \alpha_1, \ldots, \alpha_l, p_{\neq\alpha}) \tag{18}$$

Where $p_{\neq\alpha}$ denotes all model parameters other than P-velocities. Differentiating with respect to parameter $p$ gives

$$\left.\frac{\partial G_{h_l}}{\partial p}\right|_{h=const} = \begin{cases} \left.\dfrac{\partial G}{\partial P}\dfrac{\partial P}{\partial \alpha_j}\right|_{h=const} + \left.\dfrac{\partial G}{\alpha_j}\right|_{P=const} & p = \alpha_j \\ \left.\dfrac{\partial G}{\partial p_{\neq\alpha}}\right|_{P=const} & p = p_{\neq\alpha} \end{cases} \tag{19}$$

The value of $\left.\dfrac{\partial P}{\partial \alpha_j}\right|_{h=const}$ may be determined from equation (15) by setting the differential $dh_l$ equal to zero.

$$dh_l = -2\sum_{k=1}^{l-1} \frac{A_k z_k dA_k}{(A_k^2 - 1)^{3/2}} = 0 \tag{20}$$

From equation (17) the differential $dA_k$ can be evaluated.

$$dA_k = A_k\left(-\frac{dP}{P} - \frac{d\alpha_k}{\alpha_k}\right) \tag{21}$$

The differential $dh_l$ is seen to depend only on ray parameter $P$ and the P-velocities above the $l+1$-th layer. Now it is possible to evaluate the required partial derivative $g'$. If all the $d\alpha_k$ are zero except for $d\alpha_j$, equation (20) becomes

$$dh_l = dP\left(\frac{2}{P}\sum_{k=1}^{l-1} \frac{A_k^2 z_k}{(A_k^2 - 1)^{3/2}}\right) + d\alpha_j\left(\frac{2A_j^2 z_j}{\alpha_j(A_j^2 - 1)^{3/2}}\right)$$

$$= \frac{\partial h}{\partial P}dP + \frac{\partial h}{\partial \alpha_j}d\alpha_j = 0 \tag{22}$$

$$\rightarrow \quad \left.\frac{\partial P}{\partial \alpha_j}\right|_{h=const} = -\frac{\dfrac{\partial h}{\partial \alpha_j}}{\dfrac{\partial h}{\partial P}} = \frac{-PA_j^2 z_j}{\alpha_j(A_j^2 - 1)^{3/2}}\left(\sum_{k=1}^{l-1} \frac{A_k^2 z_k}{(A_k^2 - 1)^{3/2}}\right)^{-1} \tag{23}$$

Equation (23) shows how to find the partial derivative of ray parameter with respect to P-

velocity of one layer while keeping offset $h$ constant. The partial of the gather with respect to ray parameter $\frac{\partial G}{\partial P}$, can be evaluated numerically using a finite difference formula. The above two terms are plugged into equation (19) to compute $g'$. All that remains is the evaluation of the partial derivatives of gather $G$ with respect to parameter $p$. Differentiating equation (5) with respect to $p$ yields

$$\frac{\partial G_{hw}}{\partial p} =$$

$$\sum_{l=1}^{L} G_{h_l w}\left(\frac{1}{S_w}\frac{\partial S_w}{\partial p}+\frac{1}{U_{h_l w}}\frac{\partial U_{h_l w}}{\partial p}+\frac{1}{R_{h_l}}\frac{\partial R_{h_l}}{\partial p}+\frac{1}{T^{+}_{h_l}}\frac{\partial T^{+}_{h_l}}{\partial p}+\frac{1}{T^{-}_{h_l}}\frac{\partial T^{-}_{h_l}}{\partial p}\right) \qquad (24)$$

The various partial derivatives in (24) can be computed using equations (5) through (17), along with the expressions for the reflection and transmission coefficients. The required partial derivatives in equation (24) are given in the appendix.

**Numerical example**

A simple numerical test was carried out to illustrate the algorithm under ideal circumstances. The iterative inversion formula given in equation (1), with parameters Gaussian distributed about their values at the previous iteration, is

$$p_{k+1} = p_k+(g'^{T}_k C_d^{-1} g'_k + C_p^{-1})^{-1} g'^{T}_k C_d^{-1}[d-g(p_k)]$$

Diagonal forms of data and parameter covariance matrices were used so this formula becomes

$$p_{k+1} = p_k+(g'^{T}_k g'_k + \sigma_d^2\left[\sigma_p^2\right]^{-1}) g'^{T}_k[d-g(p_k)]$$

The elements in the matrix $\left[\sigma_p^2\right]$ are simply the P and S velocity variances $\sigma_{vp}^2$ and $\sigma_{vs}^2$. A synthetic common midpoint (CMP) gather was generated using the 16 layer model shown in figure 1. These model parameters are denoted by $p_{true}$. The field geometry is a 16 fold common midpoint gather with a minimum offset of 0 km and maximum offset of .4 km. The recording times were from .2 sec to .704 sec at a sample rate of .008 sec. The time sample rate of .008 seconds is approximately equivalent to the depth sample rate of layers of .008 km for a P velocity around 2 km/sec. Therefore, there is no requirement that the location of layer boundaries be known in the inversion. The gather was computed by summing the P wave primary reflection ray responses, with ray spreading neglected, so the gather represents only a somewhat unrealistic "partial ray response" of the full theoretical

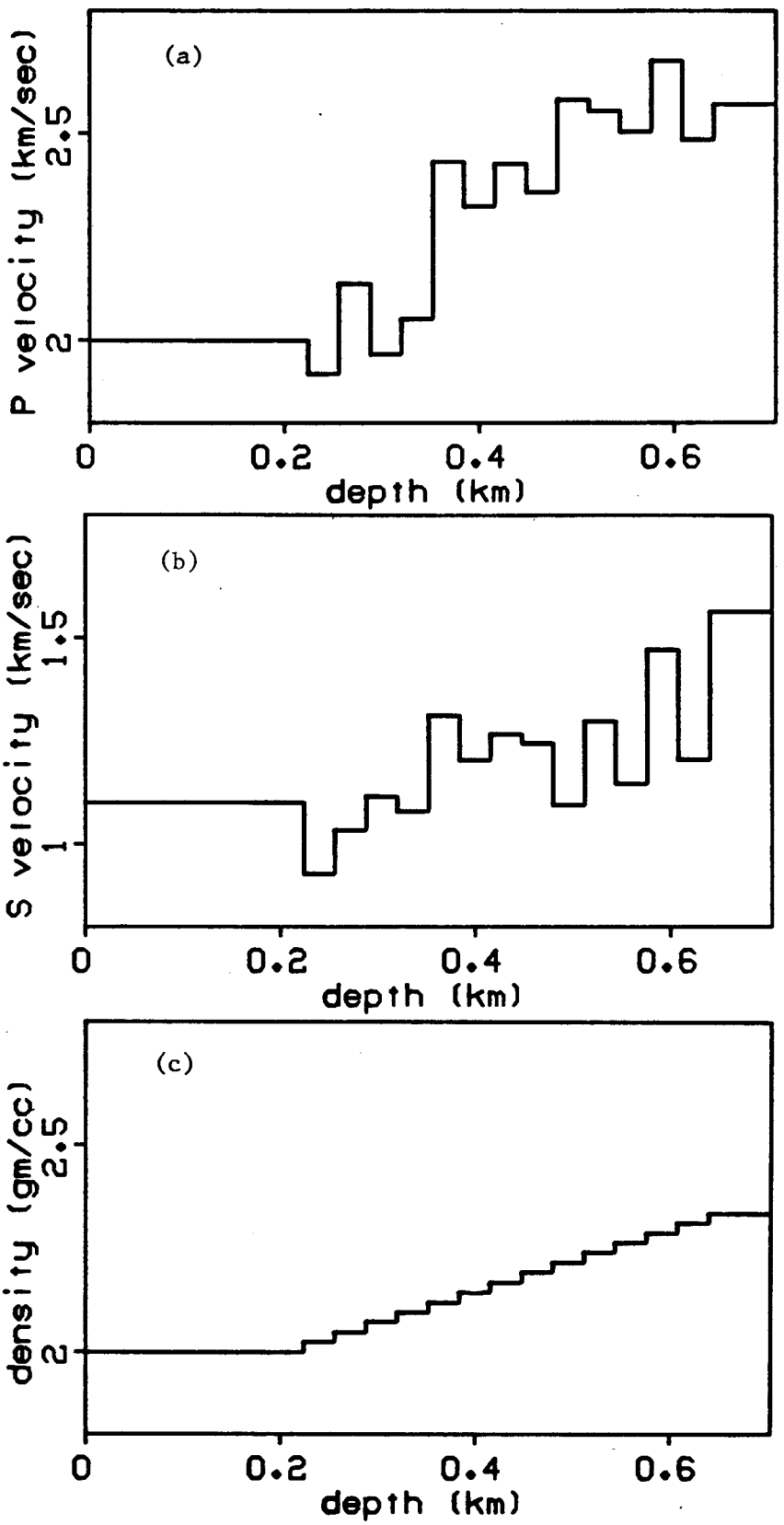


FIG. 1. 16 layer model used to generate data $d$. The layer parameters are denoted $p_{true}$. (a) P velocity model, (b) S velocity model, (c) Density model.

wavefield. The source waveform is the delayed second derivative Gaussian wavelet shown in figure 2. An isotropic source directivity pattern has been used in the modeling though inclusion of a more realistic directivity would not be difficult.

The synthetic gather or data $d=g(p_{true})$ is shown both in a perspective view and as traces in figure 3 to highlight the amplitude and phase variation with offset. These variations supply the information which allows the wavefield to be inverted for both P and S velocities even though the wavefield is composed purely of P wave primaries. The amplitude and phase variation with offset is caused by varying superposition effects resulting from increased ray traveltimes as angle through the layers increases, plus the variation of P and S wave partitioning as a function of incidence angle. The reflection coefficient has the dominant influence on the amplitude versus offset variation, while the transmission product and superposition effects are weaker. Note that the inclusion of a free surface effect on the source directivity would be seen as an extra term in the scattering coefficient product. In this simple experiment, the velocities of the uppermost layer are assumed to be known and so the free surface effect provides no additional information that would be useful in the inversion.

For the purposes of illustrating the invertibility of a CMP gather for both P and S velocity, it was assumed that the source waveform, the density for all layers, and the P and S velocities of the uppermost layer are known. The model parameters $p$ are therefore the P and S wave velocities of the 15 lower layers of the 16 layer model. The initial guess $p_0$ used for the inversion was a linear fit for the P and S velocities in the lower 15 layers as shown in figure 4.

The crucial requirement of the initial guess, is that the average P velocity never vary so far from the true average velocity that the kinematics of reflections be incorrect by more than about 1/4 of the fundamental period of the source which is the region of approximate linearity of oscillating functions. If reflections are misplaced by too much, then the inversion has little chance of succeeding because the algorithm requires that the modeled wavefield be close enough to the data wavefield so that there is approximate linearity between the two wavefields. The local minima in such optimization problems involving oscillating signals are typically spaced at about half of the fundamental period so the inversion is expected to converge to a local minima if the initial guess is so bad that events are misplaced by more than about a half-period. Tricks can sometimes be used to get out of local minima but none have been tried in this example. The other important factor crucial to the stability of the iterative algorithm is the data deviation divided by the parameter deviation $\sigma_d / \sigma_p$ which can be thought of as a damping factor. In this example, the damping factor was chosen by trial and error, such that the parameters were approximately critically damped as the iterations

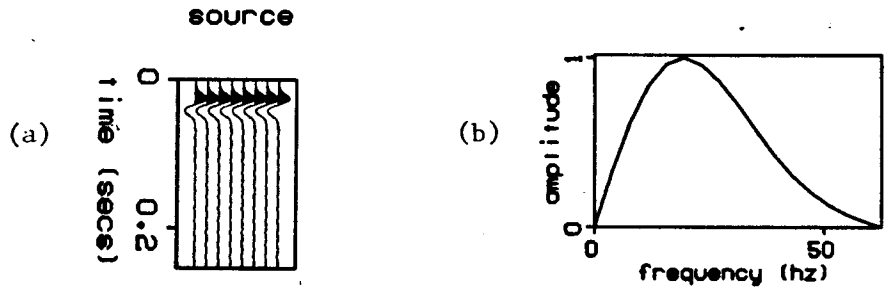


FIG. 2. Source wavelet. (a) Time domain source, (b) Source spectrum.

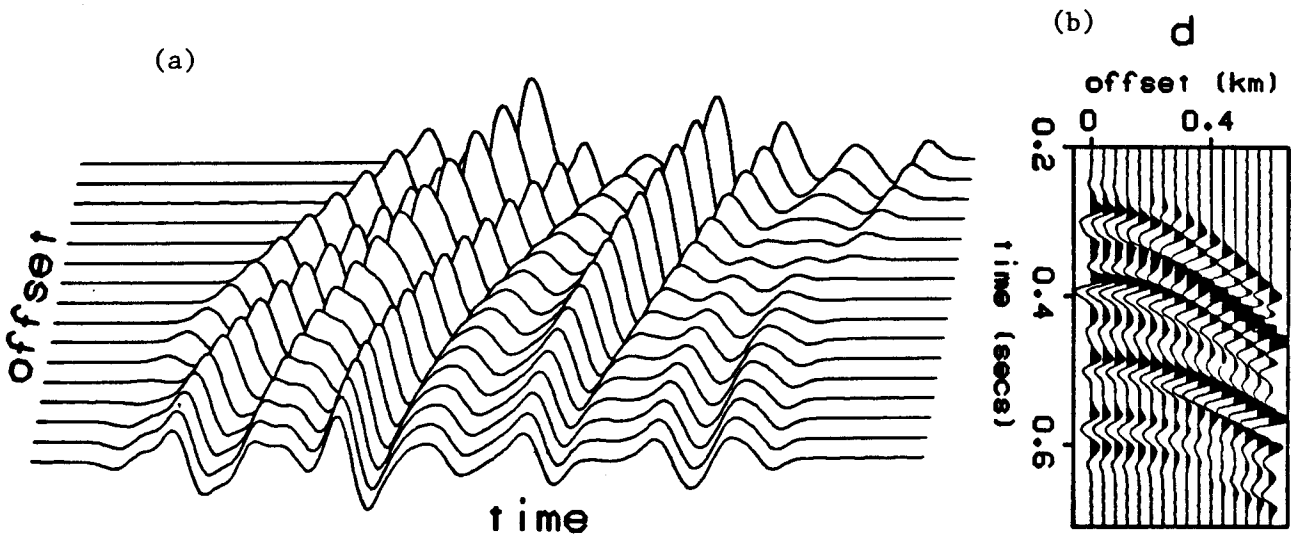


FIG. 3. The synthetic data $d$ to be inverted. (a) Data $d$ in perspective view , (b) Data $d$ as traces.

proceeded which is a safe way to ensure stability. One problem is that events are moving around slightly as P velocity varies, so nonlinearity in P velocity is much stronger than in S velocity. Hence, more damping was given to the P velocities than the S velocities so $\sigma_{vp}^{-1} > \sigma_{vs}^{-1}$. The relation used was $\sigma_{vp}^{-1} \approx 2.5\sigma_{vs}^{-1}$.

After about 16 iterations, the normalized square error $[d-g(p_k)]^T[d-g(p_k)]/(d^T d)$ was very close to zero as shown in figure 5 which indicates a best fit solution has been located for this noise free data. The P and S velocities were still changing very gradually after the 16-th iteration indicating nearness to a stationary point in the square error function. The modeled data at every fourth iteration is shown in figure 6. By the eighth iteration,

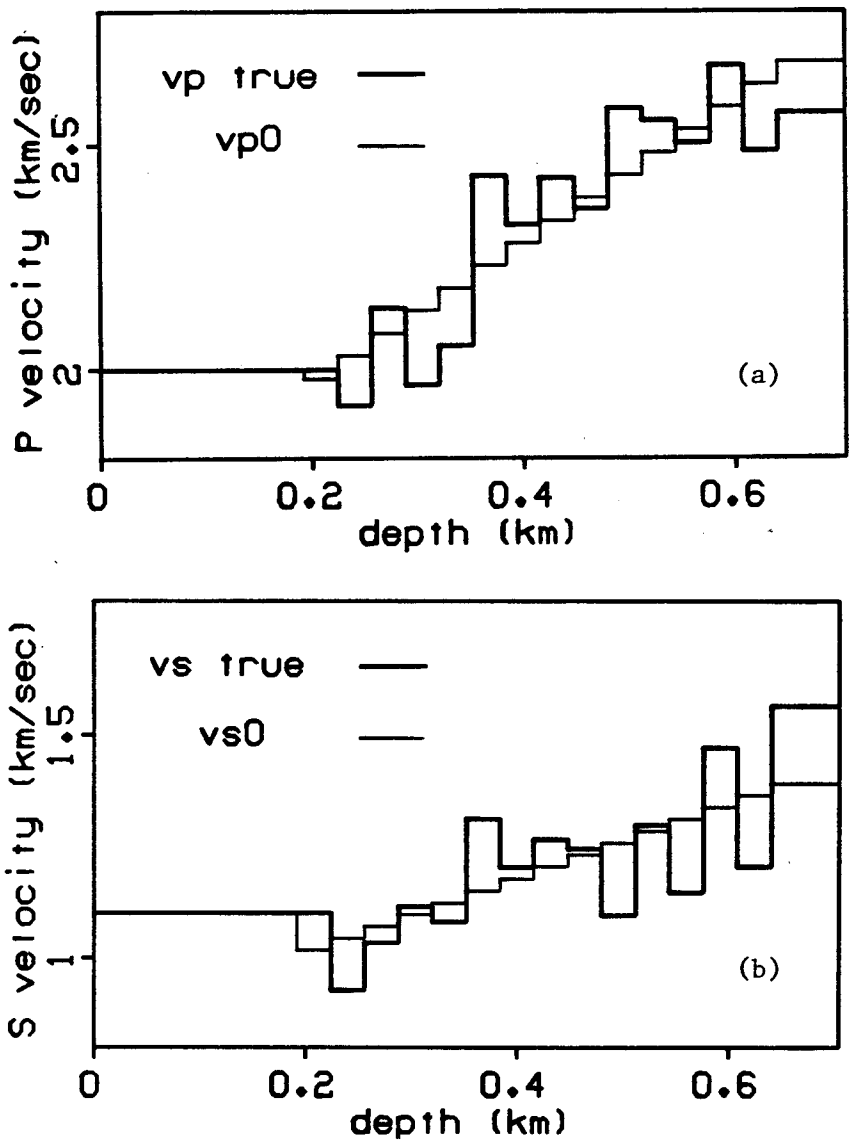


FIG. 4. The true parameters $p_{true}$ used to generate the synthetic data $d$ and the starting guess $p_0$ for the iterative inversion algorithm. (a) True P velocity and starting guess, (b) True S velocity and starting guess.

the naked eye cannot perceive significant differences between the data $d$ and the modeled data at that iteration $g(p_8)$.

Figure 7 is a plot of the difference between $d$ and $g(p)$ at every fourth iteration demonstrating that the difference between the true data and modeled data decreases as the iterative inversion proceeds. The most important test of whether the inversion is yielding a significant answer is the comparison between the true P and S velocities and those obtained from the inversion. The result is shown in figure 8 and indicates that the inversion

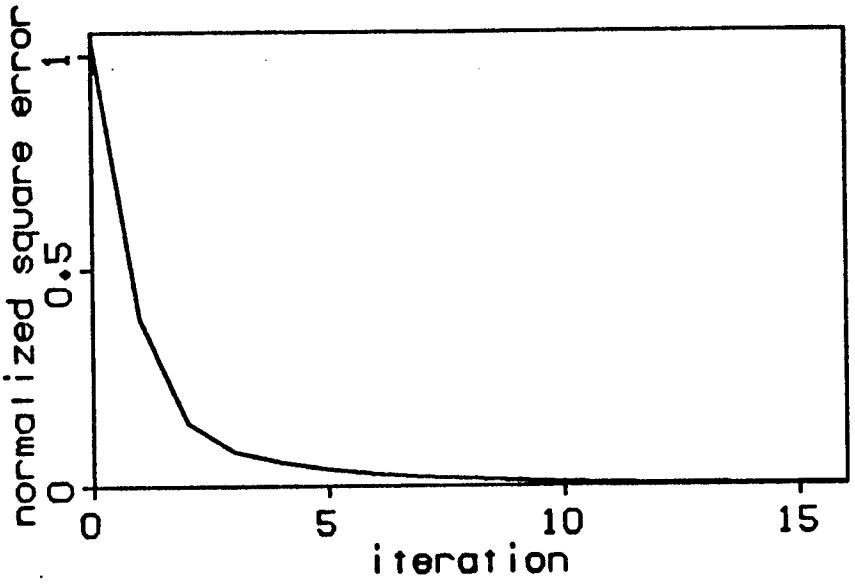


FIG. 5. Normalized square error $[d-g(p_k)]^T[d-g(p_k)]/(d^Td)$.

was successful in this simplistic synthetic test in that the P and S velocities obtained from the inversion after 16 iterations have a fair accuracy. All the velocity jumps have the correct sign and approximately the correct magnitude.

It is noteworthy that the P velocities in the lowest two layers of figure 8(a) are significantly in error though the velocity jumps are not too bad. After 16 iterations these velocities were still gradually converging. This indicates that the P velocities of these layers exert a weaker influence on the gather relative to the P velocities of the other layers and so converge more slowly. That the parameters with the strongest influence are most easily invertible is an inherent limitation of inversion. This can be stated mathematically, that there is an effective cutoff in eigenvalues of $(g'^T C_d^{-1} g' + C_p^{-1})^{-1}$ introduced by choosing $C_d$ and $C_p$. Singular value decomposition a useful tool to to study parameter sensitivities and this cutoff.

## Discussion

Results of the test case used in the previous section indicate that it is possible under ideal circumstances to invert for P and S velocities using only P wave data. The scheme is based on standard nonlinear inversion algorithms where the required partial derivatives of the modeled data with respect to the model parameters were computed during the forward

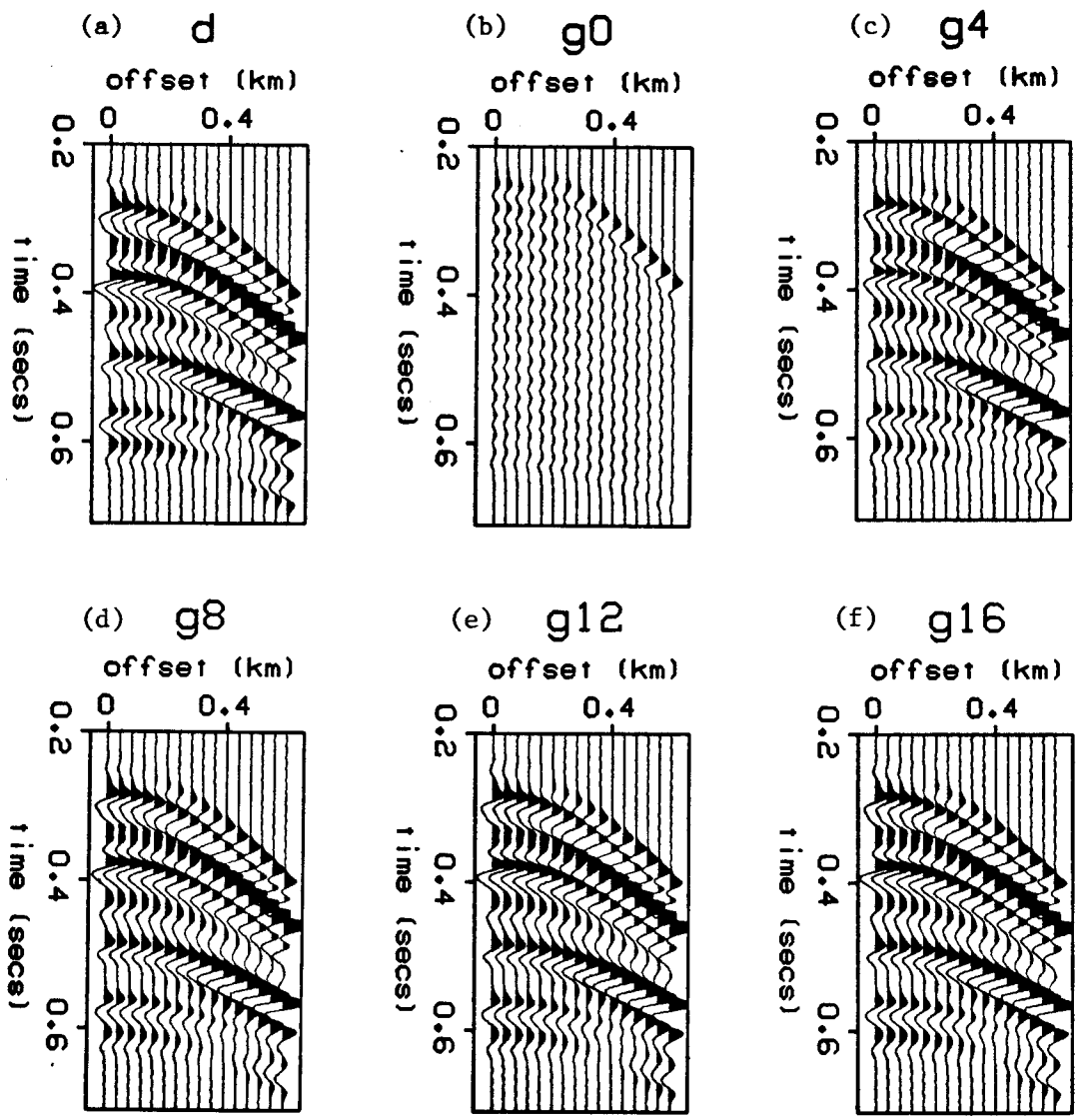


FIG. 6. True data $d$ and modeled data $g(p)$ every four iterations. (a) Data $d$, (b) $g(p_0)$, (c) $g(p_4)$, (d) $g(p_8)$, (e) $g(p_{12})$, (f) $g(p_{16})$.

modeling phase. In more realistic situations, the inversion would be far less likely to succeed for a multitude of reasons, including use of an oversimplified or inaccurate modeling scheme, assumption of an oversimplified geology, near surface effects on amplitude and traveltime for the different shots and geophones, and "noise", that is anything not allowed for. The method also requires average P velocities with reasonable accuracy which can usually be obtained in practice using conventional velocity analysis techniques. The difficulties of inversion discussed above, may be taken into consideration, but the solution is bound to degrade as noise is added and increasingly poorly constrained parameters are introduced to

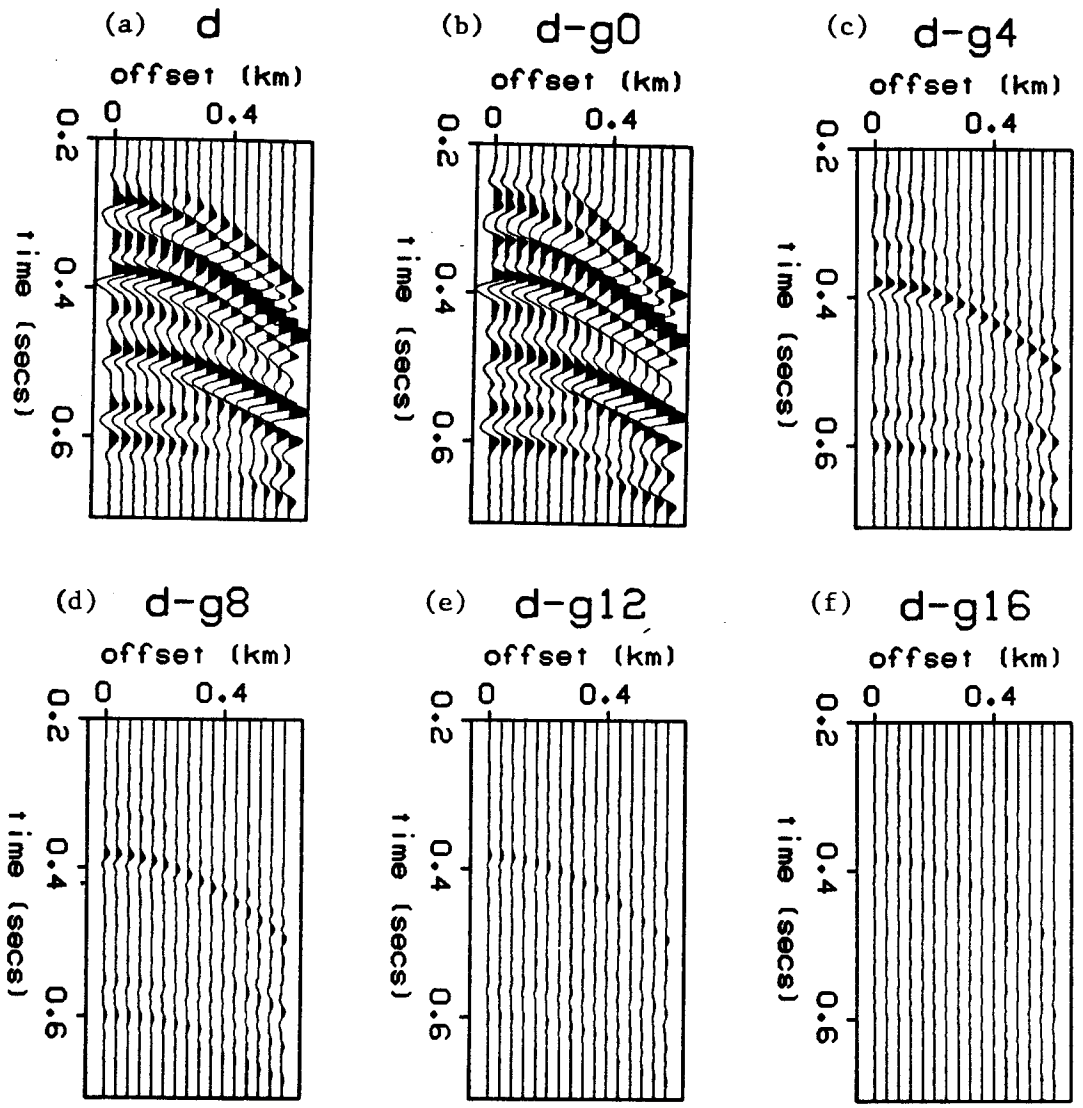


FIG. 7. True data $d$, and the difference between the true data and modeled data $d - g(p)$, every four iterations. (a) Data $d$, (b) $d-g(p_0)$, (c) $d-g(p_4)$, (d) $d-g(p_8)$, (e) $d-g(p_{12})$, (f) $d-g(p_{16})$.

refine the modeling theory.

Probably the most fundamental problem, is the use of a simplistic forward modeler. Without the intrabed and particularly near surface multiples, the modeler and hence the inversion will probably fail miserably in many real situations. However, the modeling could easily allow for multiples by summing more ray paths in the pre-existing ray theory, or by using some more sophisticated and less efficient modeling scheme such as propagator approaches. Analytic modeling methods have the advantage that the partial derivatives

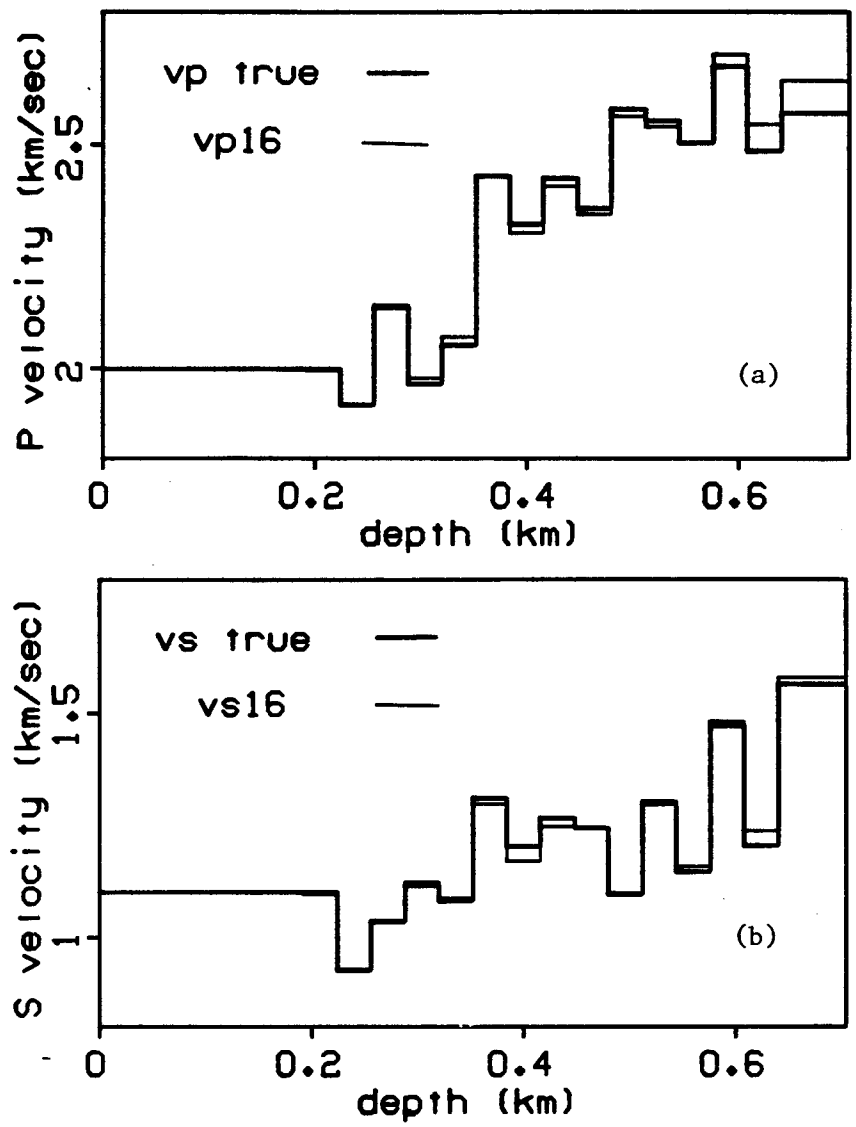


FIG. 8. True velocities $p_{true}$ and results of the inversion after 16 iterations $p_{16}$. (a) True P velocities and result of inversion after 16 iterations , (b) True S velocities and result of inversion after 16 iterations.

$\partial g_n / \partial p_m$ can be computed directly during the modeling, while numerical modeling schemes such as finite differences require some perturbation technique to obtain the approximate partial derivatives (Tarantola, 1983). The near surface effects can be included as parameters characterizing the near surface transfer function at each shot and geophone. Noise will always degrade the solution but perhaps with careful choices of $C_d$ and $C_p$ a meaningful solution can still be obtained. A more difficult problem is presented when the actual geology is more complicated than that used in the modeling scheme. A more advanced modeler capable of handling complex geology could prove to be prohibitively expensive in computer time,

and the system may become underdetermined if too many parameters are included. Use of many gathers simultaneously would help in theory, but the size of such a problem is too large for most present day computers to solve.

## Conclusions

In the ray modeling scheme outlined here, partial derivatives of the synthetic frequency domain CMP gather with respect to the model parameters are computed during the forward modeling. The model parameters are the P and S velocities, densities and quality factors of plane layers and the source waveform. Inversion may therefore be carried out using standard nonlinear least squares iterative algorithms. A numerical test is carried out where P and S velocities are inverted in a stack of 15 layers sampled at about the spatial equivalent of the Nyquist period of the CMP gather. The results of the inversion are encouraging in that both P and S velocity are inverted with reasonable accuracy.

## Acknowledgements

I wish to thanks to the fellow members of the SEP for the many interesting discussions which helped me in the creation of this paper. Special thanks to Jeff Thorson, John Toldi, Dan Rothman and Shuki Ronen. Also, thanks to Albert Tarantola and Bob Burridge for their influence and help during their brief stays at Stanford and to the SEP sponsors.

## REFERENCES

Aki and Richards, 1980, Quantitative Seismology, Freeman.

Futterman, Walter I., 1962, Dispersive Body Waves, Journal of Geophysical Research, v. 67, p. 5279-5291.

Luenberger, David G., 1973, Introduction to Linear and Nonlinear Programming, Addison Wesley.

Tarantola, Albert and Valette, Bernard, 1982, Generalized Nonlinear Inverse Problems solved using the Least Squares Criterion, Reviews of Geophysics and Space Physics, v. 20, no. 2, p 219-232.

Tarantola, Albert, 1983, Nonlinear Inverse Problem for an Heterogeneous Acoustic Medium., Pre-print submitted to Geophysics.

**APPENDIX**

$$\frac{\partial S_w}{\partial p} = \begin{cases} 0 & p \neq S_w \\ 1 & p = S_w \end{cases}$$

$$\frac{\partial U_{h_l w}}{\partial p} = \begin{cases} 0 & p \neq \alpha\,,\ p \neq Q \\ 0 & p = \alpha_j\,,\ p = Q_j \ \text{where} j > l \\ U_{h_l w} w t_{h_l j}(1 + i\delta_w)/\,Q_j^2 & p = Q_j\,,\ j \leq l \\ \dfrac{U_{h_l w} w t_{h_l w}(2 - 4P^2\alpha_j^2)[i + (1 + i\delta_w/(2Q_j))]}{\alpha_j(1 - P^2\alpha_j^2)} & p = \alpha_j \end{cases}$$

$$\frac{\partial R_{h_l}}{\partial p} = \begin{cases} 0 & p = Q\,,\ p = S \\ 0 & p = \alpha_j\,,\ \beta_j\,,\ \rho_j \ \text{where} \ j < l \ \text{or} \ j > l+1 \\ \dfrac{\partial R_{h_l}}{\partial p} & p = \alpha_j\,,\ \beta_j\,,\ \rho_j \ \text{where} \ j = l \ \text{or} \ j = l+1 \end{cases}$$

$$\frac{\partial T_{h_l}^{+/-}}{\partial p} = \begin{cases} 0 & p = Q\,,\ p = S \\ 0 & p = \alpha_j\,,\ \beta_j\,,\ \rho_j \ \text{where} \ j > l \\ \dfrac{T_{h_l}^{+/-}}{T_{h_l j}^{+/-}} \dfrac{\partial T_{h_j}^{+/-}}{\partial p} & p = \alpha_j\,,\ \beta_j\,,\ \rho_j \ \text{where} \ j = 1 \ \text{or} \ l-1 \\ T_{h_l}^{+/-}\left\{ \dfrac{1}{T_{h_l j-1}^{+/-}} \dfrac{\partial T_{h_{j-1}}^{+/-}}{\partial p} + \dfrac{1}{T_{h_l j}^{+/-}} \dfrac{\partial T_{h_j}^{+/-}}{\partial p} \right\} & p = \alpha_j\,,\ \beta_j\,,\ \rho_j \ \text{where} \ 1 < j < l-1 \end{cases}$$

The partial derivatives of the reflection and transmission coefficients can be easily computed numerically by using the centered finite difference formula $\frac{df}{dx} = \frac{f(x+\Delta x) - f(x-\Delta x)}{2\Delta x}$.

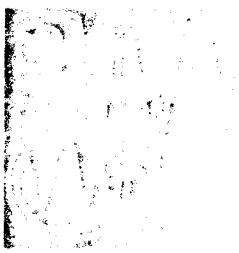

# Факультет автоматики и вычислительной техники

Декан факультета — доктор технических наук, профессор Е.Н.Браго.

Факультет создан в 1962 году.

Факультет готовит инженеров по следующим специальностям:

0606 — автоматика и телемеханика;
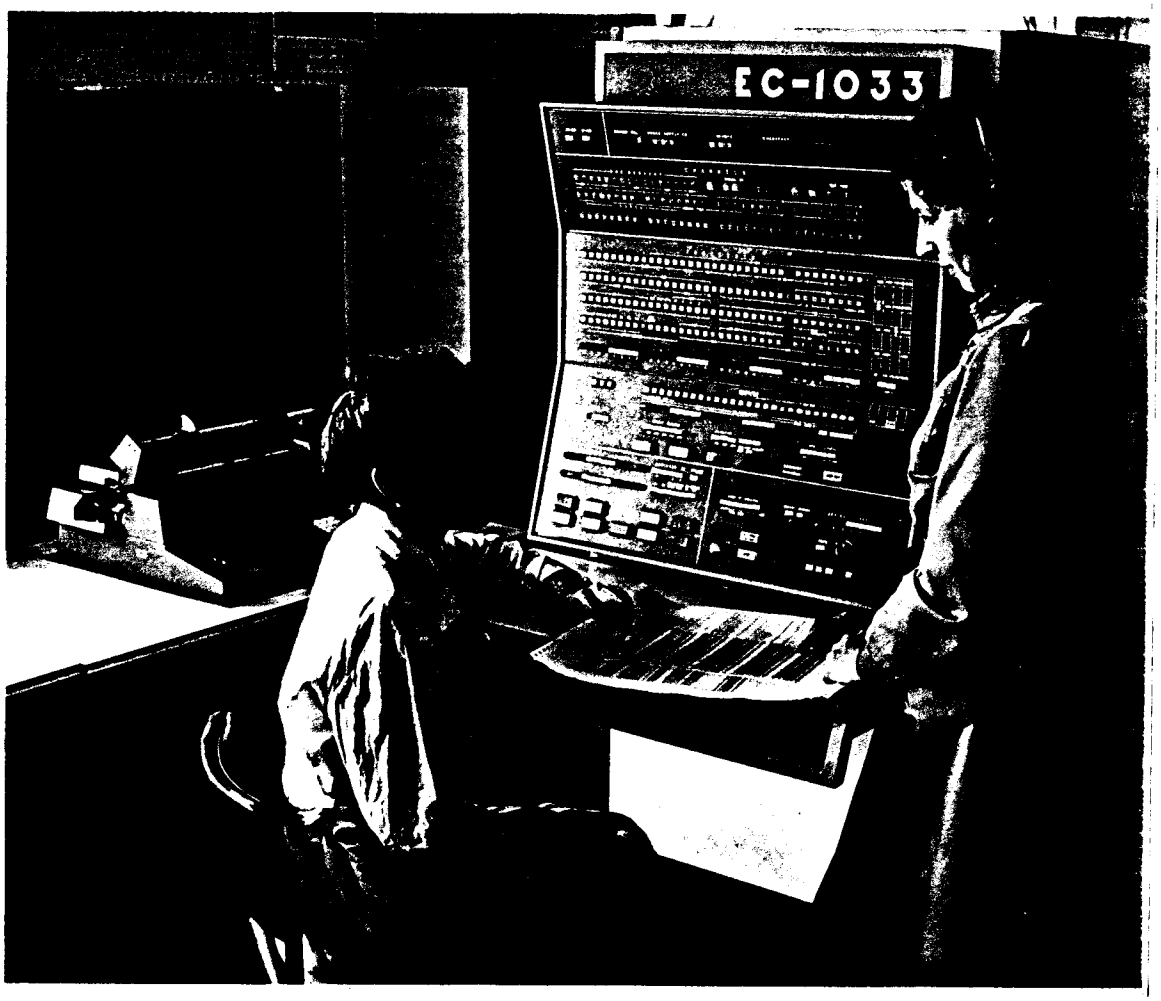
**В студенческом вычислительном зале**